Presented at 8th International Cryocooler Conference, June 28-30, Vail CO, USA

Modeling Thermal Contact Resistance

Peter Kittel

NASA Ames Research Center, Moffett Field, CA 94035-1000

ABSTRACT

One difficulty in using cryocoolers is making good thermal contact between the cooler and the instrument being cooled. The connection is often made through a bolted joint. The temperature drop associated with this joint has been the subject of many experimental and theoretical studies. The low temperature behavior of dry joints has shown some anomalous dependence on the surface condition of the mating parts. There is also some doubt on how well one can extrapolate from test samples to predicting the performance of a real system.

Both finite element and analytic models of a simple contact system have been developed. The models show that in the limit of actual contact area << the nominal area (a << A), that the excess temperature drop due to a single point of contact scales as $a^{-1/2}$. This disturbance only extends a distance ~ $A^{1/2}$ into the bulk material. A group of identical contacts will result in an excess temperature drop that scales as $n^{-1/2}$, where n is the number of contacts and n•a is constant. This implies that flat rough surfaces will have a lower excess temperature drop than flat smooth surfaces.

NOMENCLATURE

a	actual contact area ($\square\square^2$)	T	temperature
a_o	area when local yielding starts	$T_{i,j}$	temperature of element (i,j)
A	nominal contact area ($\square r_o^2$)	T_m	temperature of element (m)
A_m	Area between elements	T_o	temperature at a perfect contact
C_j	coefficient Bessel expansion of T	T_x	excess temperature
$D_{i,j}$	coefficient of generalized expansion	$T\square$	axial temperature gradient ($\partial T/\partial z$)
F	force	$T\square$	$T\square$ far from contact
F_o	force when local yielding starts	$\square T$	excess temperature
g_{2m}	Taylor expansion coefficients of $T\square$	$\square T_n$	excess temperature for n contacts
i,j,m	indices	$\square T_1$	excess temperature for 1 contact
(i,j)	i^{th}, j^{th} element	$\square T$	mean approx. excess temperature
$\mathbf{J}_0 \mathbf{J}_1$	Bessel functions	$\square T_{axial}$	approx. on axis excess temperature
k	thermal conductance	$\square T_Y$	Yovanovich's approximation
L_m	distance between elements	x	$= \square_j \square$
n	number of contacts	$\square x$	change in x
n_0	n when local yielding starts	z	axial distance from contact
Q	heat flow	z_j	$= j \square z$
Q_j	Q at $z = z_j$	z_{max}	maximum z
r	radius	$\square z$	height of toroidal element
r_i	$= i \square r$	$\square$	radius of contact
r_o	radius of cylinder	$\square_j$	constant = j^{th} zero of $\mathbf{J}_1$
$\square r$	width of toroidal element	$\square$	variance

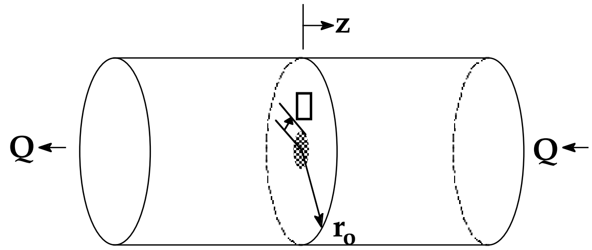

Figure 1. Diagram of a single contact between two semi-infinite cylinders. The contact is the shaded region.

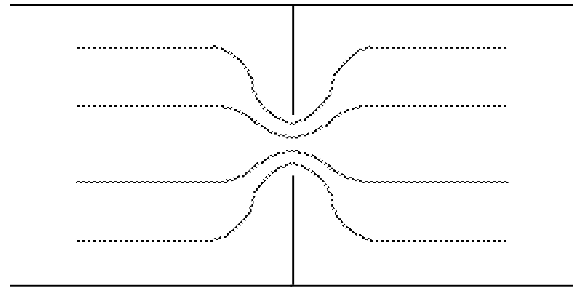

Figure 2. Representation of lines of heat flow near a constricting contact.

σ_y yield stress

INTRODUCTION

When two pieces of material are pressed together they only touch at a few small points. If heat flows across this joint the flow is constricted near these contacts. This results in a temperature difference across the joint which is bigger than for a perfect constrictionless joint. This excess temperature difference depends on the number and size of the contact points. A simple way to model this constriction is to consider a single point contact and then to extrapolate the result to a system of multiple contacts. The simplest single contact is an axisymmetric circular contact between two semi-infinite cylinders of identical material. Such a system is illustrated in Figure 1 while Figure 2 shows the effect of the constriction on the heat flow.

For further simplicity the model assumes

(a) the contact is dry (the spaces in-between the actual contact patches are perfect insulators),
(b) contacts are clean (conductivity of the actual contact is the same as the bulk),
(c) small temperature gradients (the bulk conductance is assumed to be temperature independent),
(d) the absolute temperature is low (thermal radiation effects are ignored), and
(e) the dimension, r_o, of the nominal contact area is small compared to the axial length of the bulk material (the contact effects are localized near the contact).

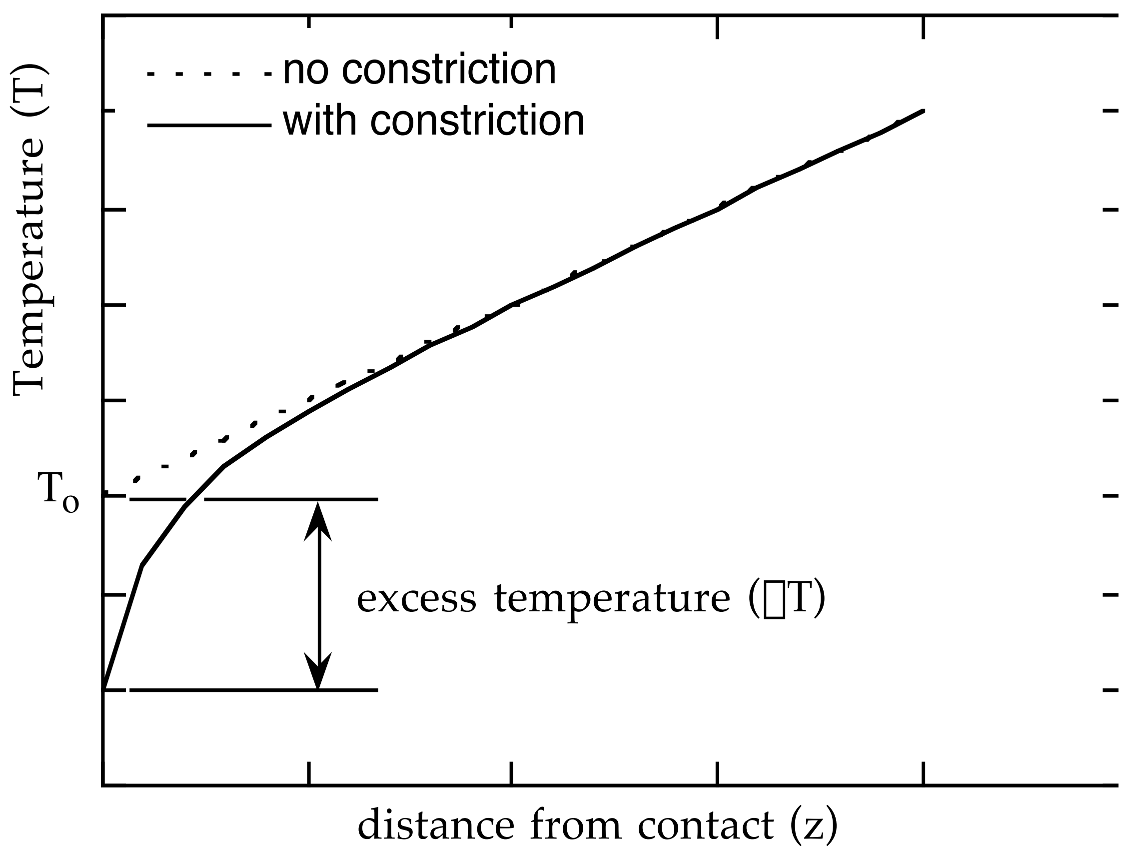

Figure 3. Temperature profile with and without the constriction due to a contact.

From symmetry, the two semi-infinite cylinders of Figure 1 are identical. The temperature profile will be symmetrical about the contact. Thus, only one of the cylinders need be considered. Figure 3 illustrates the expected temperature profile in the right semi-infinite cylinder of Figure 1.

The steady state temperature distribution is

$$\nabla^2 T = 0 \tag{1}$$

with the boundary conditions:

1) The $r = r_o$ boundary is adiabatic for all z. There is no heat flow through the side walls; i.e., $\partial T/\partial r = 0$ at $z \geq 0$, $r = r_o$.
2) The $z = 0$, $□ < r \leq r_o$ boundary is adiabatic. There is no heat transfer across the gap between the two cylinders; i.e., $\partial T/\partial z = 0$ at $z = 0$, $□ < r \leq r_o$.
3) By the symmetry of the two cylinders, the contact is isothermal; i.e., $T = T_0 + □T$ or $\partial T/\partial r = 0$ at $z = 0$, $r \leq □$.

Two approaches will be used to find a solution of this boundary value problem. The first will use a finite element model. The second will be to find an approximate analytic solution. Next, the two solutions will be compared to each other and to an earlier approximate solution.[1] Finally, some practical implications of the results will be discussed. The details of the finite element model are given in Appendix A. Appendices B,C, and D give the derivation of the analytic solution.

COMPARISON

Finite element models using three different numbers of elements were used. These were 25x76, 50x153, and 100x152 toroidal elements, where the first number refers to the radial direction and the second number to the axial direction. Both □z and □r were reduced by a factor of two for each successive model and □z = □r for all models. The contact at z = 0 was varied from a single element (□ = □z) to all elements (□ = r_o). Typical axial and radial profiles are show in Figs. 4 and 5. The figures plot normalized (dimensionless) quantities. These are $T/[r_o\ T□_\infty]$, z/r_o, and r/r_o for temperature, axial distance, and radial distance.

The axial temperature profiles in Figure 4 clearly show that the disturbance caused by the contact only penetrates a short distance into the cylinder. The disturbance is limited to the region $z < r_o$.

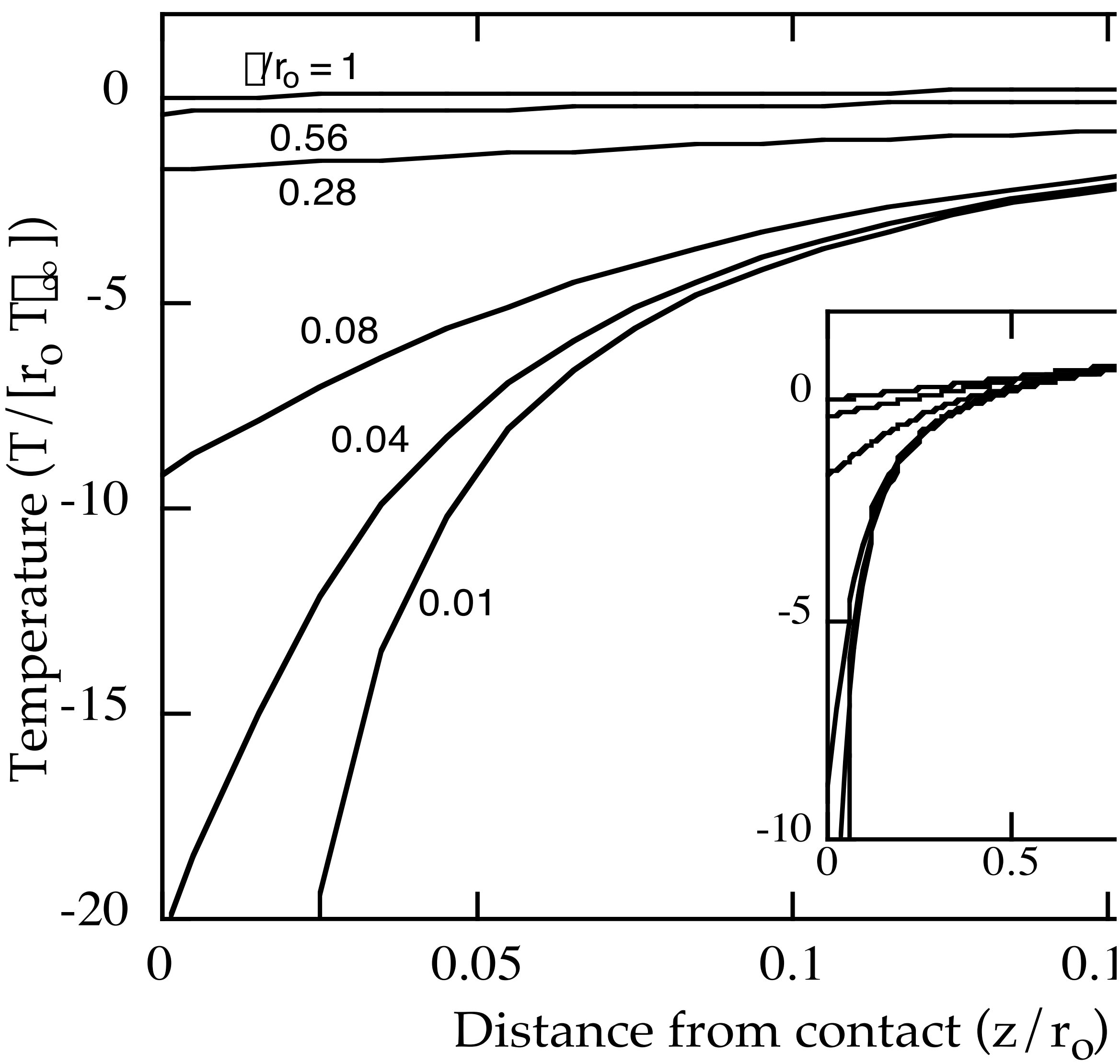

Figure 4. On axis temperature profiles for several values of □/r_o. The inset shows the same curves over an expanded range. The curves were produced by the 100x152 finite element model

This can be seen also from the analytic model. The axial dependence of Eq. (B.2) is dominated be the exp(-□$_1$z) term where □$_1 \approx 3.8/r_o$. As a result, the penetration of the disturbance is nearly independent of □. Within the $z < r_o$ region the temperature approaches the excess heat, □T, monotonically.

The radial behavior (Figure 5) also shows a dependence on □. For □/$r_o < 0.5$ and $r \gtrsim 2$□ the radial dependence appears to converge to a single function of r. For $r \leq$ □ the temperature is constant (as required by the boundary conditions) and is equal to the excess heat.

The excess heat, □T, is shown for all three finite element models in Figure 6. Also shown are the results of the analytic model and of an earlier model.[1] The differences for large □ ($\gtrsim 0.1$) between the three finite element models probably is due to several effects:

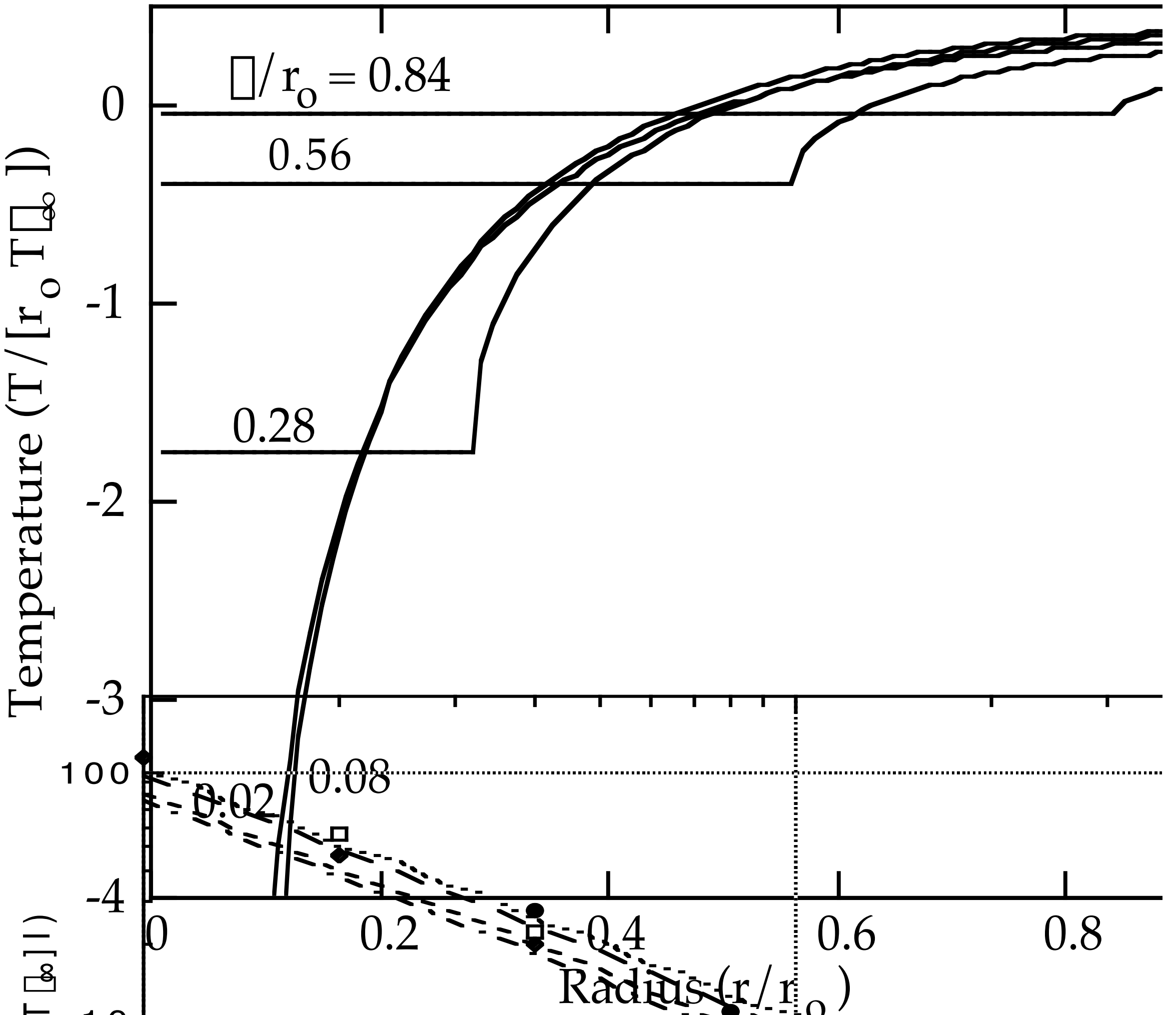

Figure 5. The contact plane (z = 0) temperature profiles for several values of □/r_o. (For □/r_o = 1 the profile would be T = 0.) The curves were produced by the 100x152 finite element model.

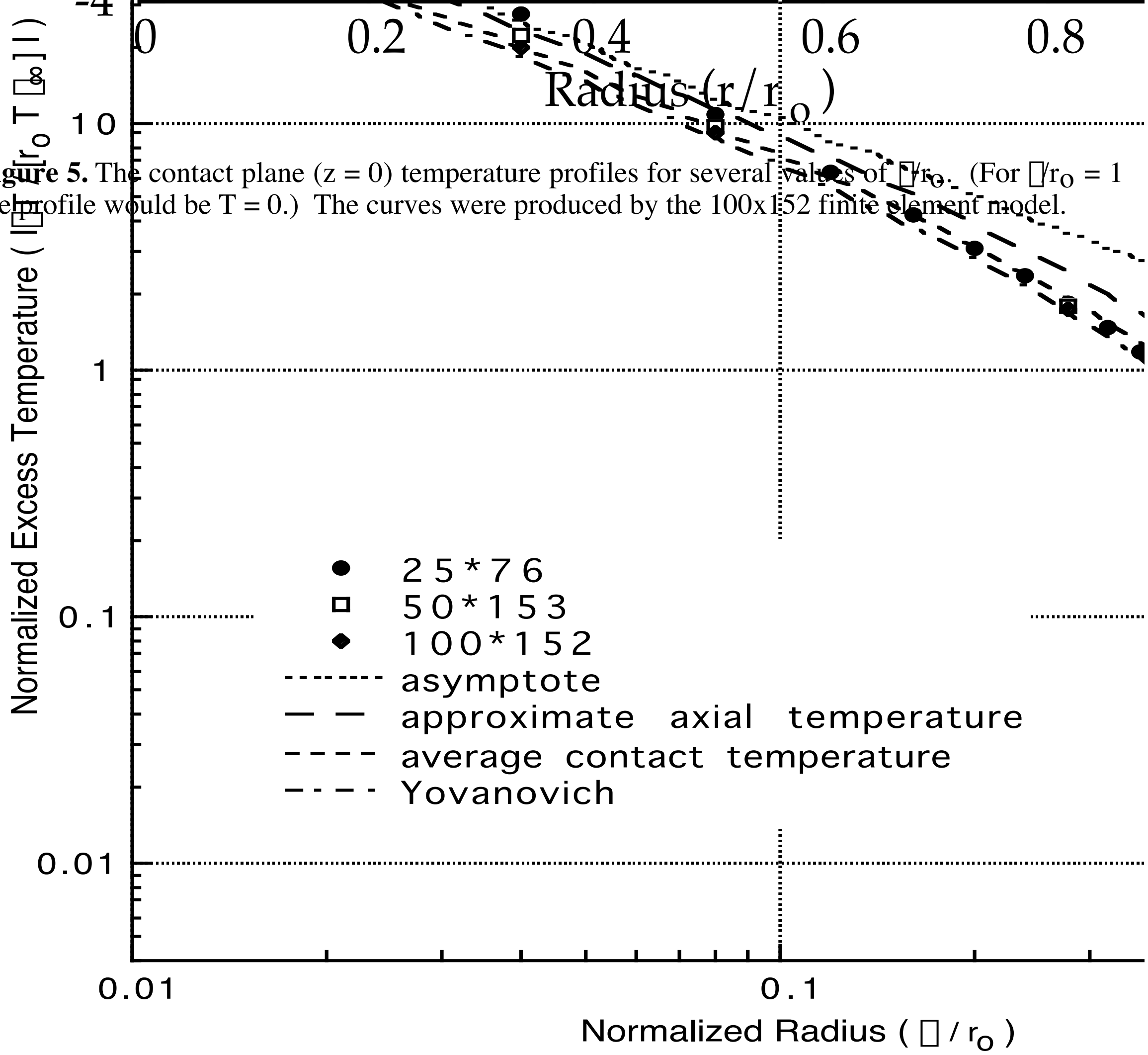

Figure 6. Excess temperature, |□T|, for all three finite element models; for the analytic expressions: Eqs, (2), (3), and (4); and the small □asymptote.

a) The model averages quantities over each element. If the quantities vary rapidly over an element, then errors are introduced. Decreasing the element size decreases this effect. In the region near z□ 0, r = □ the accuracy of the finite element model is particularly poor. In this region T and its derivatives vary rapidly.
b) Rounding errors increase as the element size decreases due to the small differences involved.
c) The convergence of the models may not be complete and may be effected by the rounding errors.

For small □ the first of these effects is particularly prevalent. Figure 6 shows that for small □, the finite element models start to deviate from each other and from the analytic models. For each of the finite element models the smallest □ used was for a contact of one element. Both Figure 4 and Figure 5 show that the derivatives of the temperature ($\partial T/\partial z$, $\partial T/\partial r$, $\partial^2 T/\partial z^2$, and $\partial^2 T/\partial r^2$) are largest near z = 0, r = □ and the derivatives increase with decreasing □. Thus, when the contact is only a few elements wide, element wide averaging no longer reflect the true behavior. In Figure 6 this deviation is noticeable only for contacts that are 3 or less elements wide.

Three analytic curves are shown in Figure 6. Two are derived in Appendix B using a model based on the Taylor series of T□ at z = 0 over $0 \le r \le$ □. Only the lowest order term of this expansion is kept. In this approximation the approximate axial temperature, Eq. (B.19), is

$$□T_{axial} = -2r_o T□ \frac{r_o}{□} \sum_{j=1} \mathbf{J}_1(□ □) \Big/ (□ _j r_o)^2 \mathbf{J}_0^2(□ _j r_o) \tag{2}$$

and the average contact temperature, Eq. (B.21), is

$$\overline{□T} = -4r_o T□ \frac{r_o^2}{□^2} \sum_{j=1} \mathbf{J}_1^2(□ □) \Big/ (□ _j r_o)^3 \mathbf{J}_0^2(□ _j r_o) \tag{3}$$

where $\mathbf{J}_1(□_j r_o) = 0$. Yovanovich assumed T□ ∝ $[1 - (r/□)^2]^{-1/2}$ and found an average temperature

$$□T_Y = -2r_o T□ \frac{r_o^2}{□^2} \sum_{j=1} \mathbf{J}_1(□ □) \sin(□ □) \Big/ (□ _j r_o)^3 \mathbf{J}_0^2(□ _j r_o) \tag{4}$$

For $r \lesssim 0.6\, r_o$, Eqs. (3) and (4) are nearly the same and are good fits to the finite element model. For larger values of r, Eq. (3) remains being a good fit while Eq. (4) significantly under predicts the excess heat.

DISCUSSION

In the limit of small □, the asymptotic behavior of the excess temperature has the form |□T/T□| ≈ r_o^2/□ (see Appendix C). This is the asymptote shown in Figure 6. The nominal contact area is A = □ r_o^2 and the actual contact area is a = □ □^{2}. Thus

$$|□T / T□| \approx A\,(□/a)^{1/2} \tag{5}$$

Now consider a system of n identical contacts uniformly distributed across a surface. Each contact has an actual contact area of a for a total actual contact area of n·a. The total nominal contact area is the whole surface, A. Each contact will give rise to an excess heat as if it had a nominal contact area of A/n. Thus, by Eq. (5), the excess heat will be

$$|□T_n / T□| \approx A/n\,(□/a)^{1/2} \tag{6}$$

If instead, there was only a single contact with the same actual contact area, n·a, and the same nominal contact area, A, its excess heat would be

$$|□T_1 / T□| \approx A\,(□/na)^{1/2} \tag{7}$$

Thus

$$□T_1 = n^{1/2}\, □T_n \tag{8}$$

The excess heat scales as $n^{-1/2}$. For the same actual contact area, many small contacts results in a smaller □T than it would for a few large contacts.

For very small forces the contact is restricted to few points (~3). Each of these points is lightly loaded at less than the yield stress. As the stress is increased, the actual contact area increases rapidly. Eventually there is local yielding at the contact points. Above the yield stress, the total contact area is

$$n \cdot a \approx (F - F_o)/□_y + n_o \cdot a_o\,, \quad \text{for } F > F_o \tag{9}$$

Thus, n·a is a linear function of the applied force. The total contact area depends only on the force, not on the number of contacts nor on the nominal surface area. Thus a rough surface which touches at many points will have a smaller □T than a smooth surface with a single contact.

This may explain some of the anomalous results that have been reported. Salerno, et.al.[2] found that for a set of brass contacts, the ones with a 0.2 and 0.4 μm finish had a factor of 2 less excess heat than contacts with 0.1, 0.8, or 1.6 μm finish. It is possible that the 0.2 and 0.4 μm samples formed more contact points. While this is not in agreement with the above suggestion that rougher is better, other factors can also influence the number of contacts. Such factors are flatness and waviness of the surface. Eventhough all the samples were nominally flat, the surface finishing process may have left some samples with a slight curvature.

In summary, finite element and analytic models of the excess temperature for a simple contact system were developed. In the limit of actual contact area « the nominal area (a « A), the excess temperature drop due to a single point of contact scales as $a^{-1/2}$. This disturbance only extends a distance ~ $A^{1/2}$ into the bulk material. A group of identical contacts will result in an excess temperature drop that scales as $n^{-1/2}$, where n is the number of contacts and n·a is constant. This implies that flat rough surfaces will have a lower excess temperature drop than flat smooth surfaces.

REFERENCES

1. Yovanovich, M.M. "General Expression for Circular Constriction Resistances for Arbitrary Flux Distributions," Progress in Astronautics and Aeronautics, vol. 49 (1976) p. 381.

2. Salerno, L.J., Kittel, P., Brooks, W.F., Spivak, A.L., and Marks Jr., W.G, "Thermal Conductance of Pressed Brass Contacts at Liquid Helium Temperatures," Cryogenics, vol. 26, (1986) p. 217.

3. Hildebrand, F.B., Advanced Calculus for Applications, Prentice-Hall, New Jersey (1962)

APPENDIX A - FINITE ELEMENT MODEL

The finite element model is quite simple. In setting up the elements, one can take advantage of the cylindrical symmetry. The cylinder is divided into a set of tori with rectangular crossections. Figure A.1 shows a typical element. For simplicity, the tori all have the same height and width. The labeling scheme for the elements is shown in Figure A.2. Where $0 \le r_i \le r_o$, $0 \le z_j \le z_{max}$, and $z_{max} > r_o$. Equation (1) can be rewritten as a thermal balance equation:

$$\sum_m \left(T_{i,j} - T_m\right) A_m / L_m = 0 \qquad \text{(A.1)}$$

where m represents the set of four nearest neighbors of element (i,j). The nearest neighbors to (i,j) are m = {(i,j+1),(i+1,j),(i-1,j),(i,j-1)}. For axial and radial neighbors respectively, A_m/L_m has the form:

$$\frac{A_m}{L_m} = \begin{cases} \pi\left(r_{i+1}^2 - r_i^2\right) \Delta z^{-1} & ; m = (i,\ j+1) \\ 2\pi r_{i+1} \Delta z\, \Delta r^{-1} & ; m = (i+1,\ j) \\ 2\pi r_i \Delta z\, \Delta r^{-1} & ; m = (i-1,\ j) \\ \pi\left(r_{i+1}^2 - r_i^2\right) \Delta z^{-1} & ; m = (i,\ j-1) \end{cases} \qquad \text{(A.2)}$$

The boundary conditions become

1) There are no elements for $r > r_o$. At this boundary the summation in Eq. (A.1) is over the three nearest neighbors.
2) There are no elements for $z < 0$, $0 \le r \le r_o$. At this boundary the summation in Eq. (A.1) is over the three nearest neighbors.
3) At the $z = 0$, $r \le$ [illegible] boundary, the

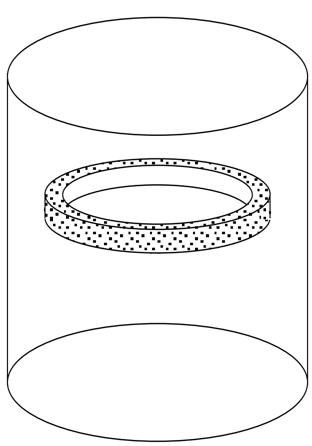

Figure A.1. Illustration of a typical element.

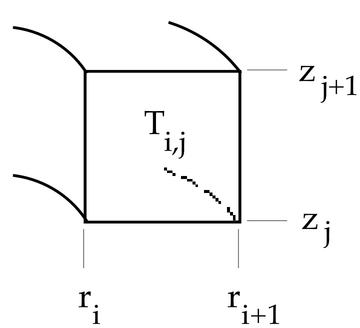

Figure A.2. Labeling scheme for elements temperature is uniform. This is acheived by placing a set of "contact" elements at $z = 0$ which are all at the same temperature. The Δz between the contact elements and the regular elements is $\Delta z/2$.

4) There are no elements for $r < 0$. At this boundary the summation in Eq. (A.1) is over the three nearest neighbors.
5) Only a finite length cylinder can be modeled by this method. The cylinder is cut off at $z = z_{max} > r_o$ and assumed to be isothermal at that surface.

Equation (A.1) can be solved for the $T_{i,j}$ by an iterative process if two additional conditions are imposed. These may be any two of the following: $T(z=z_{max})$, $T(z=0)$, or $\partial T/\partial z$ at either $z = z_{max}$ or $z \to 0$. For ease of computation, Δz and Δr are kept constant and Eq. (A.1) was written as

$$T_{i,j} = \sum_m T_m \frac{A_m}{L_m} \Big/ \sum_m \frac{A_m}{L_m} \tag{A.3}$$

Convergence was fastest if $\partial T/\partial z$ at $z = z_{max}$ was fixed and if $T(z=0)$ was adjusted after iteration to force the heat flow through the contact to equal the flow at $z = z_{max}$. The heat flow

$$Q_j = \sum_i \square \left(T_{i,j} - T_{i,j-1}\right)\left(r_{i+1}^2 - r_i^2\right)\left(\Delta z\right)^{-1} \tag{A.4}$$

is a conserved quantity. In a steady state solution, Q_j is independent of j. The Q_j at $z = 0$ and at $z \to z_{max}$ were used to determine convergence.

APPENDIX B - ANALYTIC MODEL

Equation (1) may be written in cylindrical coordinates as

$$\frac{\partial^2 T}{\partial r^2} + \frac{1}{r}\frac{\partial T}{\partial r} + \frac{\partial^2 T}{\partial x^2} = 0, \quad T = T(z, r, \square) \tag{B.1}$$

This equation may be solved by standard separation of variables techniques.[3] The general solution that is finite over all of a semi-infinite cylinder ($z \geq 0$, $r \leq r_o$) is

$$T(z, r, \square) = T_0 + T'z + \sum_{j=1} C_j \mathbf{J}_0(\square_j r) e^{-\square_j z} \tag{B.2}$$

where the C_j are only functions of $\square$. The first two terms on right hand side of Eq. (B.2) are the solution if the contact were perfect ($\square = r_o$). The last term on the right hand side of Eq. (B.2) is due to the constriction of the contact. The excess temperature is

$$\Delta T = T(0, r \leq \square, \square) - T_0 = \sum_{j=1} C_j \mathbf{J}_0(\square_j r) \tag{B.3}$$

By the boundary conditions, ΔT is only a function of $\square$. At $r = 0$, Eq. (B.3) reduces to

$$\Delta T = \sum_{j=1} C_j \tag{B.3a}$$

The boundary conditions for Eq. (B.1) may be summarized as

$$\mathbf{J}_1(\square_j r_o) = 0 \tag{B.4}$$

$$\sum_{j=1} \square_j C_j \mathbf{J}_0(\square_j r) = T', \quad \square < r \leq r_o \tag{B.5}$$

$$\sum_{j=1} C_j \mathbf{J}_0(\square_j r) = \Delta T, \quad r \leq \square \tag{B.6}$$

The first of these makes use of the relation $\partial \mathbf{J}_0/\partial r = \square_j \mathbf{J}_1$. Eq. (B.4) defines a set of discrete $\square_j r_o$ values called the zeros of $\mathbf{J}_1$. The second boundary condition comes from evaluating $\partial T/\partial z = 0$ for Eq. (B.2) at $z = 0$. The final condition is that the contact is isothermal.

The difficulty in finding an analytic solution to this boundary value problem is the mixed nature of the $z = 0$ boundary conditions. This boundary is defined in terms of T for $r \leq \square$ and in terms of $\partial T/\partial z$ for $\square < r \leq r_o$. If either T or $\partial T/\partial z$ were defined over the whole boundary, then a solution would be straight forward. The approach followed here is to find a replacement set of boundary conditions which defines $\partial T/\partial z$ over the entire $z = 0$ interface. The approach is to expand $\partial T/\partial z$ about $r = 0$ at $z = 0$. Then a boundary condition approximating the true condition will be used to find an approximate solution. Here the approximation uses only the lowest order term of the $\partial T/\partial z$ expansion. More terms could be used for greater accuracy. A means of using more terms will be outlined in Appendix D.

For simplicity of notation, let $T' = \partial T/\partial z$. Then from Eq. (B.2)

$$T' = T'_\infty - \sum_{j=1}^{\infty} \lambda_j C_j \mathbf{J}_0(\lambda_j r) e^{-\lambda_j z} \tag{B.7}$$

The conservation of energy requires that the heat flow across any z = constant plane be independent of z. In equation form, this statement may be written as

$$Q = k\, 2\pi \int_0^{r_o} T' r\, dr \tag{B.8}$$

Evaluating this at $z = \infty$ and at $z = 0$ and recalling the second boundary condition ($T' = 0$ at $z = 0$, $\square < r \le r_o$), results in

$$2\pi \int_0^{r_o} T' r\, dr = 2\pi \int_0^{\square} T'(0,r,\square)\, r\, dr \tag{B.9}$$

The integrand, T', of Eq. (B.9) may be expanded in a Taylor series over the range $r \le \square$:

$$T'(0, r, \square) = T'_\infty + \sum_{m=0}^{\infty} g_{2m}(\square)\, r^{2m} \tag{B.10}$$

where

$$g_{2m}(\square) = \frac{1}{(2m)!} \frac{d^{2m} T'(0,r,\square)}{dr^{2m}} \bigg|_{r=0} \tag{B.11}$$

The odd terms of the expansion in Eq. (B.10) vanish because of the cylindrical symmetry; i.e. $T'(z, -r, \square) = T'(z, r, \square)$. Substituting Eqs. (B.10) and (B.11) into Eq. (B.9) and evaluating the integral gives

$$r_o^2\, T'_\infty = \square^2 \left(T'_\infty + g_0\right) + \sum_{m=1}^{\infty} (2m+2)^{-1} g_{2m}(\square)\, \square^{2m+2} \tag{B.12}$$

Keeping only the lowest order terms yields

$$g_0 \approx T'_\infty \left(r_o^2 / \square^2 - 1\right) \tag{B.13}$$

where

$$g_0 = T'(0, 0, \square) - T'_\infty \tag{B.14}$$

This is a replacement boundary condition for $z = 0$ and $r \le \square$. By substituting Eqs. (B.13) and (B.14) into Eq. (B.7), the new set of boundary conditions may be written as

$$\mathbf{J}_1(\lambda_j r_o) = 0 \tag{B.15}$$

$$\sum_{j=1}^{\infty} \lambda_j C_j \mathbf{J}_0(\lambda_j r) = \begin{cases} T'_\infty \left(1 - r_o^2 \square^{-2}\right) & ; r \le \square \\ T'_\infty & ; \square < r \le r_o \end{cases} \tag{B.16}$$

Eqs. (B.15) and (B.16) are based on only the lowest order term of the expansion of $\partial T/\partial z$. The coefficient of this term, g_0, was found using an additional constraint, the conservation of energy. If higher order terms are desired then yet more constraints will be needed to find the new coefficients, g_{2m}. Appendix D contains a discussion of an approach to this problem.

Equations (B.15) and (B.16) may solved using standard Bessel function techniques,[3] yielding

$$C_j = -2 r_o T'_\infty \frac{r_o}{\square} \frac{\mathbf{J}_1(\lambda_j \square)}{(\lambda_j r_o)^2 \mathbf{J}_0^2(\lambda_j r_o)} \tag{B.17}$$

Substituting this into Eq. (B.3) gives the excess temperature:

$$T_x = -2 r_o T' \frac{r_o}{\square} \sum_{j=1}^{\infty} \mathbf{J}_1(\lambda_j \square)\, \mathbf{J}_0(\lambda_j r) \Big/ (\lambda_j r_o)^2\, \mathbf{J}_0^2(\lambda_j r_o) \tag{B.18}$$

Because Eq. (B.17) is based on an approximation of $\partial T/\partial z$ the third boundary condition, Eq. (B.6), is not met. This calculated temperature, T_x, across the contact is not constant, rather $|T_x/T'_\infty|$ is a maximum at $r = 0$ and decreases with increasing r. This is shown in Figure B.1.. The on axis ($r = 0$) value for this estimate is

$$\Delta T_{axial} = -2 r_o T'_\infty \frac{r_o}{\square} \sum_{j=1}^{\infty} \mathbf{J}_1(\lambda_j \square) \Big/ (\lambda_j r_o)^2 \mathbf{J}_0^2(\lambda_j r_o) \tag{B.19}$$

Because Eq. (B.19) represents an extrema, it over estimates the excess heat. The average value of T_x might be a more reasonable quantity to use. The average value is

$$\overline{\Delta T} = \frac{1}{\pi \square^2} \int_0^{\square} T_x\, 2\pi r\, dr \tag{B.20}$$

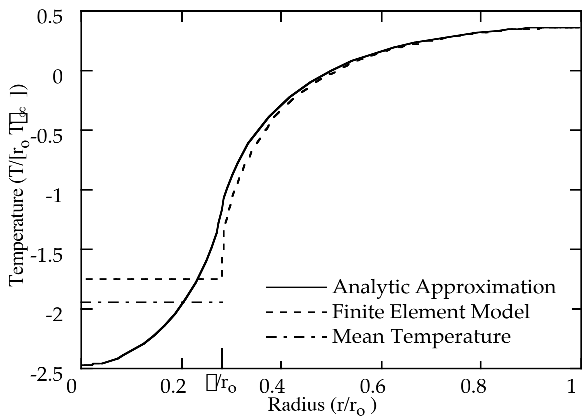

Figure B.1. Comparison of the 100*152 finite element model with the analytic approximation, Eq. (B.18), for $\square/r_o = 0.28$. Also shown is the mean temperature approximation, Eq. (B.21).

Substituting Eq. (B.18) into Eq. (B.20), integrating and using the relation $\int x\mathbf{J}_0(x)dx = x\mathbf{J}_1(x)$ yields

$$\overline{\square T} = -4r_o T\square\frac{r_o^2}{\square^2}\square_{j=1}\mathbf{J}_1^2(\square\,\square_j)\Big/(\square ƒ_o)^3\,\mathbf{J}_0^2(\square ƒ_o) \qquad \text{(B.21)}$$

APPENDIX C - ASYMPTOTIC BEHAVIOR OF □T IN THE LIMIT OF SMALL □

This appendix will derive the asymptotic behavior of □T in the limit of small □. Three similar equations have been given for □T as a function of □. These are Eqs. (B.19), (B.21), and (4):

$$\square T_{axial} = -2r_o T\square\frac{r_o}{\square}\square_{j=1}\mathbf{J}_1(\square\,\square_j)\Big/(\square ƒ_o)^2\mathbf{J}_0^2(\square ƒ_o) \qquad \text{(C.1)}$$

$$\overline{\square T} = -4r_o T\square\frac{r_o^2}{\square^2}\square_{j=1}\mathbf{J}_1^2(\square\,\square_j)\Big/(\square ƒ_o)^3\,\mathbf{J}_0^2(\square ƒ_o) \qquad \text{(C.2)}$$

$$\square T_Y = -2r_o T\square\frac{r_o^2}{\square^2}\square_{j=1}\mathbf{J}_1(\square\,\square_j)\sin(\square\,\square_j)\Big/(\square ƒ_o)^3\,\mathbf{J}_0^2(\square ƒ_o) \qquad \text{(C.3)}$$

In the limit of large j, $\mathbf{J}_0^2(\square_j r_o) \approx 2/\square\square_j r_o$ and $\square_j r_o \approx (j + 1/4)\,\square$. In the limit of small □, the summations in Eqs. (C.1), (C.2), and (C.3) can be replaced by integrations. This is done by multiplying the addend by □x/□x where $x = \square_j\square$. The upper □x becomes dx, while the lower one becomes $\square\,\square\square_j = \square\square/r_o$. Thus the three expressions for □T become

$$\square T_{axial} \sim -r_o T\square\frac{r_o}{\square}\int_0 \mathbf{J}_1(x)\,\frac{dx}{x} = -r_o T\square\frac{r_o}{\square} \qquad \text{(C.4)}$$

$$\overline{\square T} \sim -r_o T\square\frac{r_o}{\square}\int_0 \mathbf{J}_1^2(x)\,\frac{dx}{x^2}\ \square -0.85\,r_o T\square\frac{r_o}{\square} \qquad \text{(C.5)}$$

$$\square T_Y \sim -r_o T\square\frac{r_o}{\square}\int_0 \mathbf{J}_1(x)\sin(x)\,\frac{dx}{x^2}\ \square -0.78\,r_o T\square\frac{r_o}{\square} \qquad \text{(C.6)}$$

APPENDIX D - A GENERALIZED EXPANSION SOLUTION

Appendix B found a solution using the lowest order expansion of T□ at z = 0, r ≤ □. This appendix will outline a more general solution. Eq. (B.10) gives the complete expansion. If a solution of order n ($0 \le n < \infty$) is desired, then Eq. (B.10) can be written as

$$T^{\square}\left(0, r, \square\right) = T^{\square} + \sum_{m=0}^{n} g_{2m}(\square)\, r^{2m} \tag{D.1}$$

where
$$g_{2m}(\square) = \frac{1}{\left(2m\right)!} \frac{d^{2m} T^{\square}\left(0, r, \square\right)}{d r^{2m}}\Bigg|_{r=0} \tag{D.2}$$

Evaluating Eq. (B.7) at z = 0:

$$T^{\square} = T^{\square} - \sum_{j=1} \square C_j\, \mathbf{J}_0\left(\square_j r\right) \tag{D.3}$$

Recalling the boundary condition $T^{\square} = 0$ for $\square < r \le r_o$ and combining Eqs. (D.1) and (D.3), yields

$$\sum_{j=1} \square C_j\, \mathbf{J}_0\left(\square_j r\right) = \begin{cases} -\sum_{m=0}^{n} g_{2m} r^{2m} & , \ r \,\square\, \square \\ T^{\square} & , \ \square < r \,\square\, r_o \end{cases} \tag{D.4}$$

This may be written as a linear combination boundary value problems. Replacing the C_j by

$$C_j = \sum_{m=-1}^{n} g_{2m} D_{j,m} \tag{D.5}$$

where $D_{j,m}$ are defined by

$$\sum_{j=1} \square D_{j,m}\, \mathbf{J}_0\left(\square_j r\right) = \begin{cases} -r^{2m} & , \ 0 \,\square\, m \,\square\, n, \ r \,\square\, \square \\ 0 & , \ \begin{cases} 0 \,\square\, m \,\square\, n, \ \square < r \,\square\, r_o \\ \text{or} \quad m = -1, \ r \,\square\, \square \end{cases} \\ T^{\square} & , \ m = -1, \ \square < r \,\square\, r_o \end{cases} \tag{D.6}$$

and $g_{-2} \equiv 1$. Using this expansion, the excess heat, Eq. (B.3). becomes

$$T_x = \sum_{j=1} \sum_{m=-1}^{n} g_{2m} D_{j,m}\, \mathbf{J}_0\left(\square_j r\right) \tag{D.7}$$

We want $T_x = \square T$, where T_x is a function of r and $\square T$ is a constant. This can only be achieved as $n \,\square\, \infty$. The best that can be done for a finite n is to minimize the variance between the two. The variance is

$$\square = \frac{2}{\square^2} \int_0^{\square} \left(T_x - \square T\right)^2 r\, dr \tag{D.8}$$

The minimum occurs when $\partial \square / \partial g_{2m} = 0$ for all m. Applying this to Eq. (D.8) yields

$$\frac{\partial \square}{\partial g_{2m}} = \frac{4}{\square^2} \int_0^{\square} \left(T_x - \square T\right) \frac{\partial T_x}{\partial g_{2m}}\, r\, dr = 0 \tag{D.9}$$

Substituting Eq. (D.7) into (D.9), differentiating, integrating, and rearranging terms gives

$$\sum_{k=0}^{n} g_{2k} \left[\sum_{j=0} D_{j,k} \int_0^{\square} \mathbf{J}_0\left(\square_j r\right) \mathbf{J}_0\left(\square_i r\right) r\, dr \right] = \square T \frac{\square}{\square_i} \mathbf{J}_1\left(\square_i \square\right) \tag{D.10}$$

where $0 \le i \le n$. Eq. (D.10) is a set of n+1 linear equations in n+2 unknowns. The unknowns are the n+1 g_{2k} and $\square T$. A final condition is the conservation of energy, Eq. (B.12):

$$T^{\square} \left(\frac{r_o^{\,2}}{\square^2} - 1 \right) = \sum_{m=1}^{n} \left(2m + 2\right)^{-1} g_{2m}\, \square^{2m} \tag{D.11}$$

Solving this set of equations, Eqs, (D.10) and (D.11), will give the $n^{\underline{th}}$ order approximation for T_x and $\square T$.